Research article

Journal of Physical Organic Chemistry

Received: 19 May 2015, Revised: 13 November 2015, Accepted: 16 November 2015, Published online in Wiley Online Library: 22 December 2015

(wileyonlinelibrary.com) DOI: 10.1002/poc.3526

Complex formation of pyridine-azacrown ether amide macrocycles with proton and heavy metal ions in aqueous solution

Yury Fedorov[a,c]*, Olga Fedorova[a,b], Alexander Peregudov[a], Stepan Kalmykov[c,d], Bayirta Egorova[c], Dmitry Arkhipov[a], Anastasia Zubenko[a] and Maxim Oshchepkov[a,b]

This research concerns the analysis of the proton and metal ion binding of amide macrocycles of different structures and sizes by potentiometric, ^{1}H NMR and X-ray diffraction methods. Protonated ligands exist as a 3D network structures. The ligands form 1:1 complexes with heavy metal ions (Cu^{2+}, Cd^{2+}, Pb^{2+}, Zn^{2+}, and Ni^{2+}) in aqueous solutions and demonstrate the high selectivity towards Cu^{2+} cations. The pyridine-2,6-dicarbamide fragment provides structural rigidity to crown ether, resulting the molecule has an open cavity and faster kinetics of metal complexes formation.

Keywords: pyridine-azacrown ether compounds; complex formation; NMR-spectroscopy; potentiometric titration method; X-ray analysis

INTRODUCTION

Polyazamacrocyclic ligands have been extensively investigated because of their ability to form complexes with different metal ions or anionic species with considerable potential in such areas as catalysis, modeling of metalloenzyme, molecular recognition.[1–4] Because most of the applications of macrocycles are associated with their ability to form complexes with ions, the main goal in macrocyclic ligand design is to synthesize compounds that are able to discriminate between ions. The metal ion selectivity is influenced by the nature, arrangement of donor atoms and also the ring size.[5] There is at present a need for the investigation of selective coordination properties in novel systems suitable for particular practical purposes.

This paper presents the synthesis of a novel amide macrocycles **1–4** (Scheme 1), the potentiometric, ^{1}H- NMR, and X-ray structural analysis and the binding properties towards transition and heavy metal cations. Taking into account the peculiar structural characteristics of amide macrocycles, they may exhibit a range of interesting and potentially useful molecular recognition properties. However, only one example concerning the Fe^{2+} complex of amide macrocycle has been reported earlier.[6,7]

Amide macrocycles **2–4** can be easily prepared with high yields by a reaction of the corresponding diamine and dimethyl pyridine-2,6-dicarboxylate.[8] From a structural point of view, these receptors derive from the α,ω-diamine containing oxygen or nitrogen heteroatoms able for metal ion binding and pyridine residue as additional coordination center. The presence of the crown-ether moieties in the composition of receptors confers them a certain degree of flexibility that is however limited by the presence of a relatively rigid chelate subunit containing a pyridine group. Due to synthetic availability amide macrocycles are potentially applicable as ligand for heavy and transition metal ions. The information on this topic has not been found before in literature. To study the role of amide group on the complex formation, we compare the obtained data for ligand **2** for those for ligand **1**.

RESULTS AND DISCUSSION

Amidopyridine macrocycles **2–4** (Scheme 1) have been prepared by the modified method described previously.[6–8] The protonation constants of **1–4** and stability constants of its complexes with Cu^{2+}, Cd^{2+}, Pb^{2+}, Zn^{2+}, Ni^{2+}, and Fe^{2+} were determined by potentiometric methods. The values of the stability constants for the metal complexes of **1–4** studied in this work, determined in water, are compiled in Table 1.

Macrocycle **2** has one pyridine center for proton coordination; the value of its protonation constant is low enough ($\log \beta = 1.9$). Ligand **1** showed the ability to coordinate three protons. Firstly,

* *Correspondence to: Yury Fedorov, A. N. Nesmeyanov Institute of Organoelement Compounds of Russian Academy of Sciences, Vavilova, 28, Moscow, 119991, GSP-1, Russia.*
E-mail: fedorov@ineos.ac.ru

a *Y. Fedorov, O. Fedorova, A. Peregudov, D. Arkhipov, A. Zubenko, M. Oshchepkov*
A. N. Nesmeyanov Institute of Organoelement Compounds, Russian Academy of Sciences, Vavilova, 28, Moscow 119991, GSP-1, Russia

b *O. Fedorova, M. Oshchepkov*
Mendeleev University of Chemistry and Technology of Russia, Miusskaya sqr., 9., 125047, Moscow, Russia

c *Y. Fedorov, S. Kalmykov, B. Egorova*
Department of Chemistry, M. V. Lomonosov Moscow State University, Build. 3, 1 Leninskie Gory, 119991, Moscow, Russia

d *S. Kalmykov*
NRC "Kurchatov Institute", Akademika Kurchatova sqr., 1, Moscow 123182, Russia

Journal of Physical Organic Chemistry

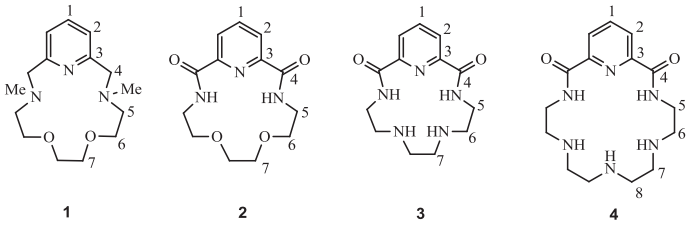

Scheme 1. Structures and numbering of the atoms of the compounds **1–4**

the protonation of macrocyclic N atoms occurs with formation of stable forms **1**·H^+ (log $\beta = 9.25$) and **1**·$(H^+)_2$ (log $\beta = 17.00$). The third hydrogen atom coordinates with pyridine residue to form **1**·$(H^+)_3$ (log $\beta = 18.9$).

Ligands **3** and **4** have five and six basic centers, respectively, but only two constants have been determined by the potentiometric technique. Compounds **3** and **4** exhibit relatively high value for the first protonation constant and moderate (in case of 3) or fairly high (in case 4) values for the second. Based on the observation described for ligands **1** and **2,** we can suggest that in Compounds **3** and **4** the protonation of aliphatic N atoms only proceeds leading to the formation of species with high enough stability (Table 1).

Single-crystals of **4**, **3**·$HClO_4$ and **4**·$(HClO_4)_2$ suitable for X-ray determination were grown from MeCN solutions at room temperature (Figs 1–7 and S1 and quantum-chemical calculations in the Supporting Information). The pyridine-2,6-dicarbamide fragment is responsible for structural rigidity of crown ether, thereby leading to open cavity.

This preorganization of the macrocycle positively effects on the process of complexation with metal cations, because there are no additional energy for conformational macrocycle transformation before complex formation.

The size of macrocyclic cavity in **4** can be estimated by the N…N distance measurements: N1…N4 5.525(3) Å, N2…N5 5.618(3) Å, N3…N6 5.438(3) Å, N3…N5 4.840(3) Å (Fig. 1(a)). Conformation of cycle **4** is shown in Fig. 1(b) along the median plane of the pyridine-2,6-dicarbamide fragment; deviations of N atoms from the plane are equal to: N3 0.319(4) Å, N4 0.620(4) Å, N5 −0.990(4) Å.

The pyridine-2,6-dicarbamide fragment in **4** is nearly flat; torsion angles N1–C1–C2–N2 and N1–C12–C11–N6 are equal to 1.7(3)° and 2.3(3)°, respectively (Fig. 1(b)). It is known[6], that this fragment in Compound **3** is not planar (corresponding torsion angles are equal to 11.87° and −9.19°, respectively). To analyze this structural feature, quantum chemical calculations of isolated molecules **3** and **4** were carried out (see detailed description in the Supporting Information).

The pyridine-2,6-dicarbamide fragment in **3** is twisted (corresponding torsion angles are equal to 4.69° and −6.49°), while in **4** it is nearly planar (−0.17° and 0.99°). This fact could be explained by the steric hindrance caused by the relatively small size of the macrocyclic ring **3** compared with **4**. It should be noted that molecules **3** and **4** are more planar in the gas phase compared with crystal. That distinction is caused by the crystal packing effects. Geometrical parameters of amide groups in structure **4** completely match those in **3**[6]

Table 1. Protonation and stability constants (log β) of the complexes of **1–4** with divalent metal ions, 25.0°C, $\mu = 0.10$ mol dm^{-3} in KNO_3

Cation	R, nm	Species	log β			
			1[5]	**2**	**3**	**4**
H^+		$[L H_3]^{3+}$	18.9 ± 0.1	—	—	—
		$[L H_2]^{2+}$	17.00 ± 0.02	—	11.8 ± 0.1	15.4 ± 0.6
		$[L H]^+$	9.25 ± 0.02	1.9 ± 0.08	8.2 ± 0.1	8.6 ± 0.4
Ni^{2+}	0.069	$[L Ni H_{-2}]$	[a]	[a]	−9.7 ± 0.2	−13.4 ± 0.2
		$[L Ni H_{-1}]^+$			−1.7 ± 0.2	−1.7 ± 0.2
		$[L Ni]^{2+}$			5.5 ± 0.2	6.0 ± 0.1
Cu^{2+}	0.073	$[L Cu H_{-2}]$	—	—	−4.0 ± 0.1	−2.8 ± 0.9
		$[L Cu H_{-1}]^+$	5.1 ± 0.1	—	5.4 ± 0.2	5.7 ± 0.5
		$[L Cu]^{2+}$	12.98 ± 0.06	—	8.8 ± 0.2	10.8 ± 0.6
		$[L Cu H]^{3+}$	—	—	—	15.4 ± 0.4
Zn^{2+}	0.074	$[L Zn H_{-3}]^-$	[a]	[a]	−22.24 ± 0.07	
		$[L Zn H_{-2}]$			−11.58 ± 0.07	−11.9 ± 0.1
		$[L Zn H_{-1}]^+$			−3.6 ± 0.1	−3.5 ± 0.07
		$[L Zn]^{2+}$			3.9 ± 0.1	4.1 ± 0.2
Fe^{2+}	0.078		[a]	[a]	[a]	
Cd^{2+}	0.095	$[L Cd H_{-3}]^-$	—	—	−23.9 ± 0.2	—
		$[L Cd H_{-2}]$	—	—	−11.9 ± 0.1	−13.04 ± 0.08
		$[L Cd H_{-1}]^+$	—	—	−3.3 ± 0.1	−3.68 ± 0.07
		$[L Cd]^{2+}$	9.96 ± 0.04	—	3.6 ± 0.5	4.2 ± 0.1
Pb^{2+}	0.119	$[L Pb H_{-2}]$	−11.38 ± 0.07	—	−13.2 ± 0.1	−13.5 ± 0.1
		$[L Pb H_{-1}]^+$	0.26 ± 0.06	—	−2.12 ± 0.03	−2.77 ± 0.05
		$[L Pb]^{2+}$	10.11 ± 0.04	—	—	4.93 ± 0.06

[a]The formation of precipitates of hydroxyl complexes prevents the potentiometric analysis.

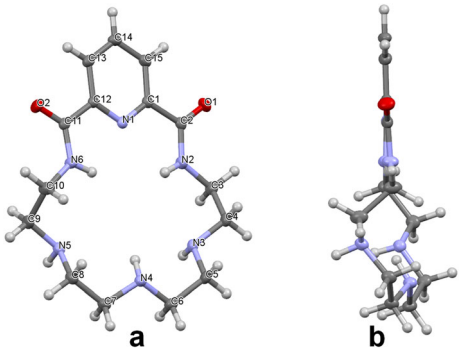

Figure 1. General view of **4**, thermal ellipsoids are drawn at the 50% probability level. MeCN molecule is omitted for clarity

(C = O 1.225(3)−1.232(3) Å, C-N 1.333(3)−1.338(3) Å, C_{amide}-C_{Py} 1.507(4)−1.515(4) Å).

The molecules of **4** form stacks by π…π interaction between the pyridine-2,6-dicarbamide fragments (plane-to-plane distance 3.330(4) Å) and N–H…N bonds (N3…N4 3.178(3) Å). Two adjacent stacks are organized in a herringbone manner (Fig. 2) due to the C–H…O contacts (C14…O2 3.312(3) Å).

Recently, another polymorph of **3**·$HClO_4$ at 293 K was described.[9] Unlike the published structure in which H-atom is distributed between two amine nitrogen atoms, in the crystal structure of **3**·$HClO_4$ at 120 K, the H-atom is localized at N3 (Fig. 3). Comparison of macrocycle conformation in different polymorphs of **3**·$HClO_4$ is shown in Fig. 4.

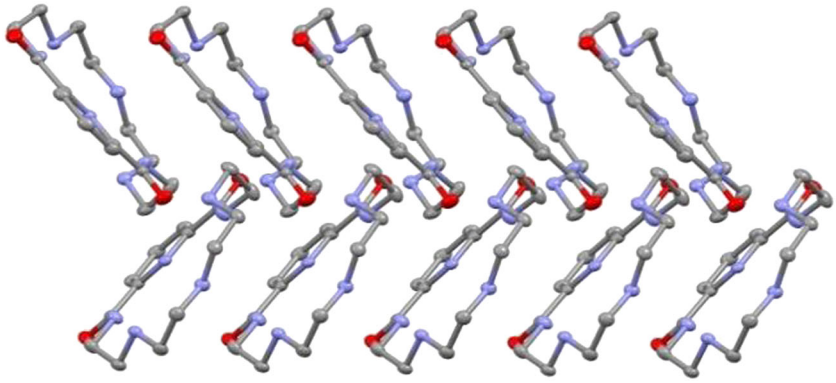

Figure 2. Crystal packing of **4**, MeCN molecules and hydrogens are omitted for clarity

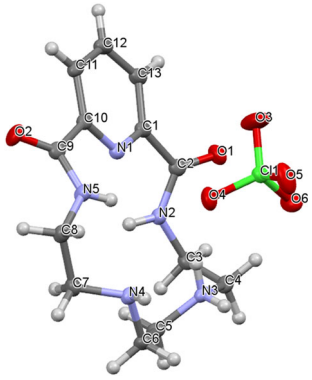

Figure 3. General view of **3**·$HClO_4$, thermal ellipsoids are drawn at the 50% probability level

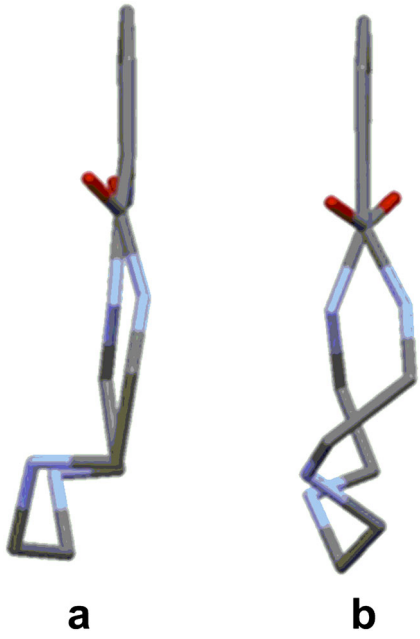

Figure 4. Macrocycle conformation in **3**·$HClO_4$, (a) – at 293 K and (b) – at 120 K. View along the pyridine ring plane, hydrogens are omitted for clarity

The pyridine-2,6-dicarbamide fragment in **3**·$HClO_4$ is strongly twisted (torsion angles N1–C1–C2–N2 and N1–C10–C9–N5 are equal to 29.5(4)° and 23.2(4)°, respectively, Fig. 4(b)) due to N–H…O bonding with perchlorate anions. These interactions lead to cation–anion columns (Fig. 5(a)), which are bound by the N–H…O bonds and C–H…O contacts (Fig. 5(b)).

Interaction between crown ether **4** and perchloric acid results in diprotonated product **4**·$(HClO_4)_2$. In contrary to the solution, in the crystal of **4**·$(HClO_4)_2$ at 120 K, the H-atoms are localized at the N3 and N5 atoms (Fig. 6(a)).

The pyridine-2,6-dicarbamide fragment in **4**·$(HClO_4)_2$ is slightly twisted; torsions N1–C1–C2–N2 and N1–C12–C11–N6 are equal to 11.4(2)° and −13.8(2)°, respectively. The macrocycle has folded conformation, angle between N6–N1–N2 plane and N6–N5–N4–N3–N2 mean plane equals to 140.14(7)°. The geometry of amide groups is the same as for **4** and **3**·$HClO_4$. The large number of H-bonds in structure of **4**·$(HClO_4)_2$ forms a 3D network (Fig. 7).

Thus, the crystals show that in both compounds **3**·$HClO_4$ and **4**·$(HClO_4)_2$ pyridine N-atom is not involved into coordination with proton. One or two protons seem to bond with donor N-atoms of the ligands **3** and **4** similarly to what we suggested from potentiometric data.

For the determination of complex formation constants, solutions of perchlorates of various metals and ligands **1–4** with different concentrations of the components were titrated with NaOH. The complex formation constants were calculated using Hyperquad software.[10] During the determination of stability constant values, the protonation constants for ligand **4** were fixed, and the formation constants of the hydroxy species were considered as known, and no attempts were made to adjust their values. In the study of metal ion

Journal of Physical Organic Chemistry

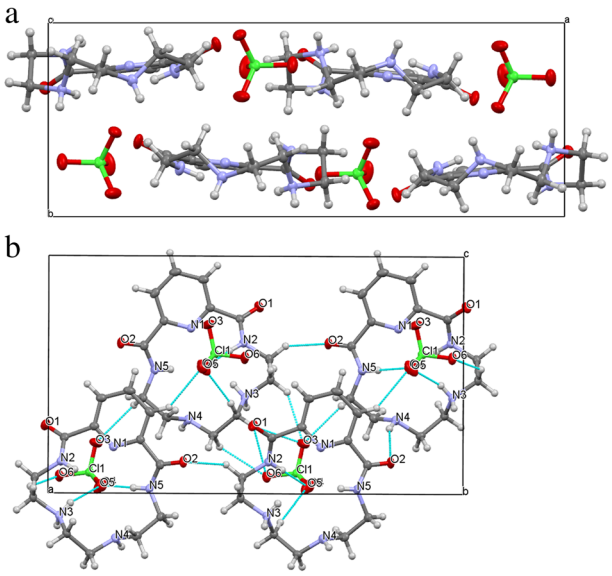

Figure 5. Crystal packing of **3**·$HClO_4$: (a) – along the *c*-axis and (b) – along the *b*-axis

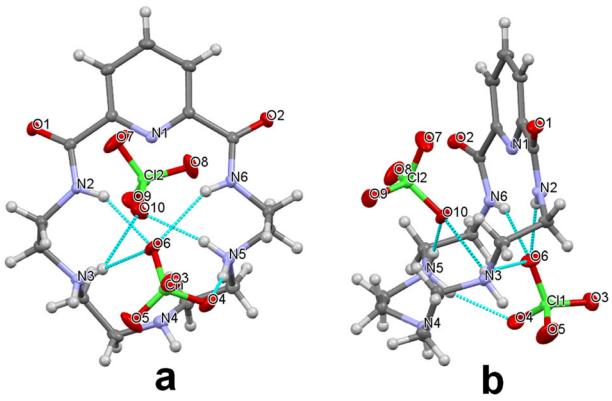

Figure 6. General view of **4**·$(HClO_4)_2$, thermal ellipsoids are drawn at the 50% probability level, second parts of disordered perchlorate anions are omitted for clarity

complexation with ligands **1–4,** the formation of hydroxy species with limited solubility in water hamper equilibrium constant determination. For Fe^{2+} and ligands **1–4**, Ni^{2+}or Zn^{2+} and ligands **1**, **2** a precipitate formation made impossible to obtain reliable constants for the ML or ML(OH) species. The potentiometric titration curves are presented in Figs S2–S27 in the Supporting Information. In all cases, hydroxy complexes of different compositions are founded, while for Cu^{2+} M(HL) species are also obtained. All ligands form complexes ML, except the case of ligand **3** interactions with Pb^{2+} when only the hydroxyl complexes are observed.

The values presented in Table 1 show that the complexes of the divalent metal ions with ligands **3** and **4** are less stable relative to those for ligand **1**. At the same time, the complex formation of ligand **2** with metal ions has not been determined. As only pyridine can coordinate with cations, we can conclude that it is not sufficient for ion's binding. The introduction of amide group into the macrocycles also decreases the ability of ligand to coordinate cations.

Within the series of studied metal ions Zn^{2+}, Cd^{2+}, and Pb^{2+}, the values of the stability constants are relatively close, while strong coordination was observed for Ni^{2+}; and in case of Cu^{2+}, the highest values of stability constants were found. It is also important that increasing of the number of aliphatic N-atoms that are able to interact with cations from two (in **3**) to three (in **4**) leads to remarkable increase of complex stability.

The ^1H and ^{13}C NMR spectra of ligands **1–4** with Pb^{2+}, Cd^{2+}, and H^+ in D_2O solution were collected and analyzed (Figs S28–S48 and Table S2, S3 in the Supporting Information). These complexes were chosen because they demonstrate spectra of good quality for analysis. The spectra were assigned on the basis of 2D ^1H,^1H COSY, HMQC, and HMBC experiments.

Coordination of the Pb^{2+} ions to **1** resulted in a downfield shift of the aliphatic and pyridine protons as compared with the free ligand (Fig. 8). This was most noticeable for H(1) and H(2), which shifted from 7.79 and 7.33 ppm to 8.09 and 7.62 ppm, respectively in **1**·Pb^{2+}.

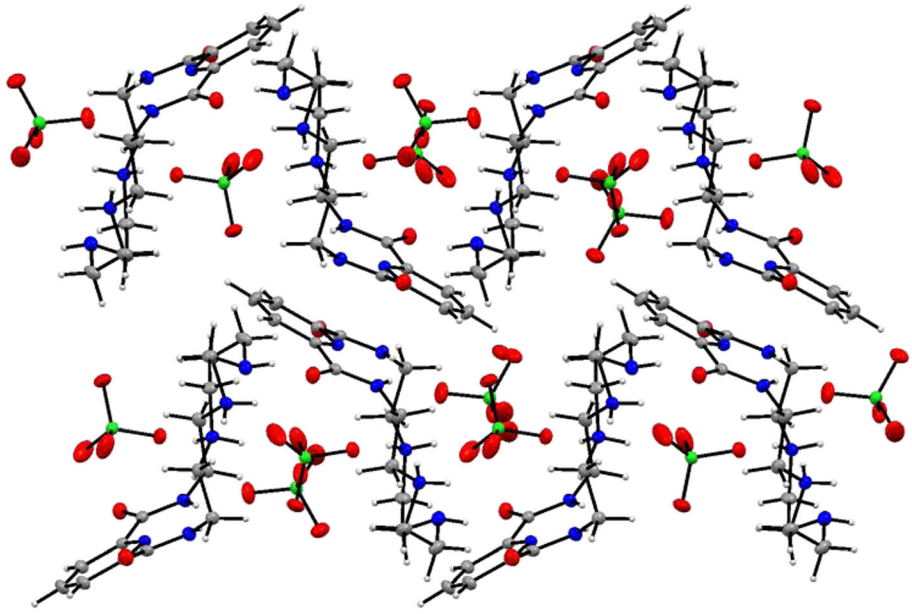

Figure 7. Crystal packing of **4**·$(HClO_4)_2$, second parts of disordered perchlorate anions are omitted for clarity

The signal H4/H4′ methylene protons showed germinal coupling, as a result of the protons being in different chemical environments, as one of the methylene protons was orientated toward one of the other ligands of the plane of the ring, while the other pointed out away from the plane of the ring. The methylene protons H(4)/H(4′) yield an AB spin pattern ($^2J_{4,4'} = 15.7$ Hz) in the ^1H NMR spectrum, while the protons of the crown moiety give AA′BB′ spin patterns (Fig. 8). This is indicative of a relatively rigid structure of **1**·Pb^{2+} in solution, probably because of the presence of bonding interactions between the metal ion and nitrogen and oxygen atoms of the crown moiety.

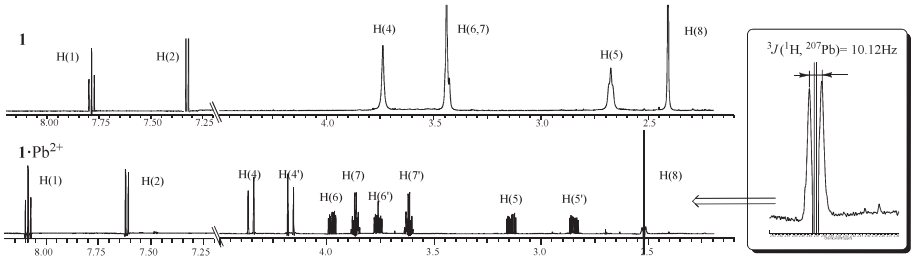

Figure 8. ^{1}H NMR spectra of **1** and 1·Pb^{2+} in D_2O, 600 MHz

Thus, the asymmetric position of the metal ion inside the macrocyclic cavity induces chirality in **1** (Scheme 2).

Changes in NMR spectrum observed upon the addition of Cd^{2+} to **1** demonstrate the formation of two conformers of complex **1**·Cd^{2+} in ratio 3:2 (Fig. S36 in the Supporting Information). The values of couple constants between ^{1}H and $^{111(113)}$Cd are $^3J(^1H, ^{111(113)}Cd) = 7.92$ MHz and $^3J(^1H, ^{111(113)}Cd) = 10.12$ MHz. Similar to Pb^{2+}, the addition of Cd^{2+} to ligand **1** causes the formation of chiral **1**·Cd^{2+}complex.

Changes in the positions of resonance signals induced by addition of $Pb^{2+}$and Cd^{2+} to the solution of **3** and **4** clearly showed the difference in structures between complexes of **3**, **4,** and **1**. According to Fig. 9, the most pronounce changes in **3**·Pb^{2+} were observed for macrocyclic proton signals in **3**; whereas, the shifting of aromatic proton signals is not remarkable (for **3**·Cd^{2+} Figs S39, S40 in the Supporting Information). Thus, the more strong coordination of Pb^{2+} and Cd^{2+} takes place through the binding of metal cations with aliphatic N-atoms of macrocycle of **3**.

Similar conclusion can be carried out for complexes **4**·Pb^{2+} and **4**·Cd^{2+} (Figs S45–S48 in the Supporting Information). Another difference between **1** and compounds **3,** and **4** is that in case of ligands **3** and **4** the metal induced chirality has not been found.

Scheme 2. Stereoisomers of **1**·Pb^{2+}

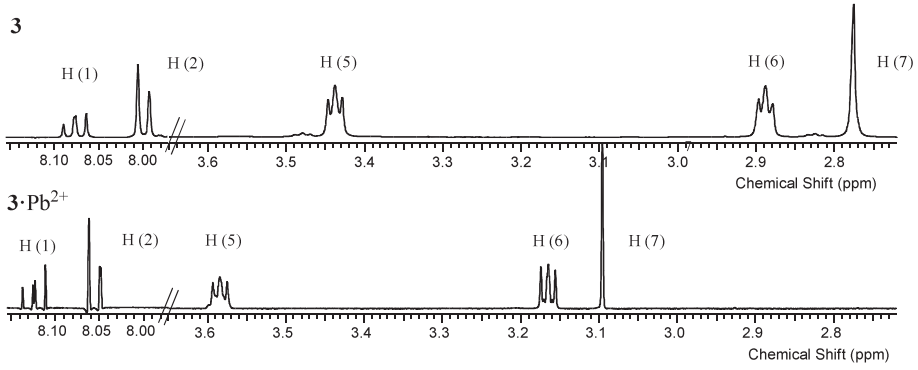

Figure 9. ^{1}H NMR spectra of **3** and **3**·Pb^{2+} in D_2O, 600 MHz

CONCLUSIONS

These studies have revealed that amide macrocycles behave as receptors for heavy metal cations and demonstrate the selectivity towards the Cu^{2+} cations. The Cu^{2+} selectivity of ligands **1**, **3**, and **4** can be interpreted taking into account the characteristics of the different ligands **1**, **2,** and **3** here considered. Thus, small different in values of stability constants of Cu^{2+} complexes with ligands **1**, **2,** and **3** points out on suitable size of ligands to coordinate a single Cu^{2+} ion involving three or four nitrogen donors. In case of ligand **1**, these are the nitrogen atoms of pyridine residue and two N-atoms of macrocyclic moiety. Obviously, that in ligands **2** and **3** N-amide atoms do not participate in coordination with Cu^{2+} cation. Similar to protonation, only macrocyclic N-atoms bind Cu^{2+}.

X-ray diffraction analysis and potentiometric data showed that in macrocycles **3** and **4** the proton coordination occurs mainly through the interaction with N-atoms of aliphatic fragments. Protonated ligands **3** and **4** form a 3D network structures. In opposite, according NMR observation in water solution, metal ions interact with N-pyridine heteroatom as well as with N-atoms of aliphatic fragments of macrocycle.

In case of ligand **1**, the metal complexes with Pb^{2+} and Cd^{2+} can function as chiral building units. Their stereoisomers in labile metal complexes are generated as a racemate coexisting in water solution. From our knowledge, this is the first example of cation-induced chirality observed for azacrown ether ligands. The example of divalent transition metal complexes with chiral N,O chelate Schiff-bases and heterocyclic azine ligands were early described.[11–14]

In spite of forming less stable complexes than those of amine macrocyclic compounds containing pyridine,[15,16] amide macrocyclic ligands demonstrate structural rigidity to crown ether due to the presence of the pyridine-2,6-dicarbamide fragment, resulting the molecule has an open cavity and faster kinetics of formation of metal complexes. Other advantages of some properties of amide macrocycles are water solubility, easy synthetic, and purification procedures. Amide macrocycles can be used as platforms to obtain N-substituted lariat ligands. The introducing of additional coordination groups will improve the binding properties of the amide macrocycles.

EXPERIMENTAL SECTION

Materials

Compound **3**,12-dimethyl-6,9-dioxa-3,12,18-triazabicyclo[12.3.1]-octadeca-1 (18),14,16- triene (1) was prepared as described earlier.[17] Analytical grade $Cu(ClO_4)_2 \cdot 6H_2O$, $Cd(ClO_4)_2 \cdot H_2O$,$Pb(ClO_4)_2 \cdot 3H_2O$, $Zn(ClO_4)_2 \cdot 6H_2O$, $Ni(ClO_4)_2 \cdot 6H_2O$, $Fe(ClO_4)_2 \cdot H_2O$ and $HClO_4$ 70% aqueous solution (Aldrich), KNO_3, NaOH (Chimmed, Russia) were used as received. All reagents and solvents were purchased from commercially

available sources and used as received.

Electrospray mass spectrometry was performed on a Finnigan LTQ instrument.

The IR spectra were recorded on a Frontier (Perkin Elmer) spectrometer using the KBr tablet method at 20 ± 1°C.

Melting points were determined on a «Mel-temp II».

All reactions were monitored for completion by thin layer chromatography performed on silica gel plates DC-Alufolien Kieselgel 60 F_{254}.

General procedure for the synthesis of macrocyclic amides

Compounds **2–4** were synthesized following the modified literature procedures.[18]

Method A

A solution of dimethyl pyridine-2,6-dicarboxylate (0.51 mmol) in 5 ml of anhydrous methanol and a solution of α,ω-diamine (0.51 mmol) in 5 ml of anhydrous methanol were simultaneously added dropwise to a solution of 5 ml of methanol containing sodium or potassium carbonate (2.25 mmol) upon intensive stirring for 40 min. The reaction mixture was kept under stirring at room temperature for 7 days. The solvent was evaporated in vacuum, and the residue was dissolved in water and extracted with chloroform (3 × 20 ml). The organic solvent was removed in vacuum to obtain the final product after recrystallization from acetonitrile.

Method B

Synthesis was carried out in the same manner without the addition of sodium carbonate (or potassium carbonate). The product can be isolated by the following ways: after the completion of the reaction, the solvent was evaporated in vacuum, and the residue was dissolved in water and extracted with chloroform (3 × 20 ml); the organic solvent was removed in vacuum to obtain the final product after recrystallization from acetonitrile.

6,9-Dioxa-3,12,18-triazabicyclo[12.3.1]octadeca-1(18),14,16-triene-2,13-dione (**2**) was obtained as white crystals. The yield was 77% (Method A). Mp is 175–180°C.[8]1

H-NMR (400 MHz, $CDCl_3$, 25°C): 3.64 (q, 4H, H(5), J = 5.0), 3.72 (t, 4H, H(6), J = 5.0), 3.74 (s, 4H, H(7)), 8.02 (t, 1H, H(1), J = 7.9), 8.24 (d, 2H, H(2), J = 7.9), 8.83 (br.s, 2H, CONH).

3,6,9,12,18-Pentaazabicyclo[12.3.1]octadeca-1(18),14,16-triene-2,13-dione (**3**) was obtained as white crystals. The yield was 74% (Method B). Mp is 211–213°C.[7,9]1

H-NMR (400 MHz, $CDCl_3$, 25°C): 2.84 (s, 4H. H(7)), 2.95 (t, 4H, H(6), J = 5.3), 3.5 (q, 4H, H(5), J = 5.3), 8.0 (t, 1H, H(1), J = 7.6), 8.23 (d, 2H, H(2), J = 7.6), 9.11 (br.s, 2H, CONH). ^{13}C-NMR (400 MHz, $CDCl_3$, 25°C): 39.3 (5-C), 47.9 (6-C), 50.0 (7-C), 124.1 (2-C), 139.5 (1-C), 148.9 (3-C), 163.3 (4-C).

3,6,9,12,15,21-Hexaazabicyclo[15.3.1]henicosa-1(21),17,19-triene-2,16-dione (**4**) was obtained as white crystals. The yield was 62% (Method B). Mp 140–142°C.

^{1}H-NMR (400 MHz, $CDCl_3$, 25°C): 2.76 (m, 4H,.H(8), J = 5.2), 2.26 (t, 4H, H(7), J = 5.2), 2.90 (t, 4H, H(6)), J = 5.2), 3.63 (q, 4H, H(5)), J = 5.2), 7.99 (t, 1H, H(1), J = 7.8), 8.34 (d, 2H, H(2), J = 7.8), 8.69 (br.t, 2H, CONH). ^{13}C-NMR (400 MHz, $CDCl_3$, 25°C): 38.7 (5-C), 49.0 (6-C), 49.7 (7-C), 50.4 (8-C), 124.9 (2-C), 138.7 (1-C), 149.0 (3-C). 163.5 (4-C).

Electrospray ionization mass spectrometry, *m/z*: 321.5 $[MH]^+$. Found (%): C, 56.21; H, 7.57, N, 26.20. $C_{15}H_{24}N_6O_2$. Calculated (%): C, 56.23; H, 7.55; N, 26.23. IR (KBr), n /cm^{-1}: 3423 (NH), 2811 (CH); 1668 (C = O); 1531 (CNH), 1442 (CH-Py).

Standard solutions

Approximately 0.1 M stock solutions of all metal perchlorates were prepared in deionized water (18.2 MΩ). $Cu(ClO_4)_2 \cdot 6H_2O$, $Cd(ClO_4)_2 \cdot H_2O$, $Pb(ClO_4)_2 \cdot 3H_2O$, $Zn(ClO_4)_2 \cdot 6H_2O$, $Ni(ClO_4)_2 \cdot 6H_2O$, $Fe(ClO_4)_2 \cdot H_2O$ solutions were standardized by complexometric titration with EDTA and using xylenol orange as indicator.[19]

A carbonate-free solution of the titrant, NaOH (≈0.1 M), was prepared with deionized water that was boiled and purged with argon while cooling to ensure removal of CO_2. This solution was standardized potentiometrically with potassium hydrogenphthalate dried at 120°C using the Gran's method and computer program GLEE[20] for the evaluation of the titration end point. Standard $HClO_4$ solution was prepared similarly by diluting the 70% product and was standardized with the NaOH described previously. Stock ligand solutions (≈0.01 M) were prepared using deionized water.

Potentiometric equipment and measurements

All potentiometric titrations were made with a Titrando 808 autotitrator equipped with a Cole Parmer combined hydrogen electrode (model 60061) and water jacketed titration vessel maintained at 25.0 ± 0.1°C with a Cole-Parmer circulating bath. The combined hydrogen electrode was calibrated as a hydrogen-ion concentration probe by titration of previously standardized amounts of $HClO_4$ with CO_2-free NaOH solution and determining the equivalent point by the Gran's method using the program GLEE,[20] which gives the standard electrode potential, E^0, and the slope, s. The ionic product of water pKw = 13.78 at 25.0°C in 0.1 mol/dm^3 KNO_3[21] was kept constant.

The potentiometric equilibrium measurements were performed in 20 ml of ligands **1–4** solutions initially between 0.001–0.002 and $HClO_4$ 0.005–0.009 mol/dm^3, first in the absence of metal ions and then in the presence of the metal ions for which [L]:[M+] ratios vary between 1.3:1 and 2: 1. Titration solutions were magnetically stirred and thermostatted at 25.0 ± 0.1°C in a water-jacketed vessel. The ionic strength of the solutions in the cell was adjusted to 0.1 mol/dm^3 with KNO_3. The electromotive force values were measured after addition of 0.0100 ml increments of standard NaOH solution. Data were collected in the pH range 2.5–10.5. A minimum of two replicates were performed.

The protonation constants of the ligands **1–4** and the stability constants of the complexes were calculated from the electromotive force titration data with the Hyperquad program.[10]

NMR spectroscopy

^{1}H NMR, ^{13}C NMR spectra were measured on a Bruker DRX-400 and Bruker DRX-600 NMR spectrometers and referenced to the residual solvent peak (^{1}H $\delta(CHCl_3)$ = 7.27 ppm, $\delta(D_2O)$ = 4.75 ppm) or to the solvent peak (^{13}C $\delta(CDCl_3)$ = 77.2 ppm). Proton signal assignments were made by first-order analysis of the spectra and analysis of 2D 1H-1H correlation maps (COSY). The spectra were assigned on the basis of 2D ^{1}H-^{1}H COSY, HMQC, and HMBC experiments.

The solution of azacrown ether ligands **1–4** (10.7 mmol) in 3 ml D_2O was mixed with a solution of lead perchlorate, cadmium

perchlorate or perchloric acid (10.7 mmol) in 3 ml D_2O. The resulting aqueous solution of the complex was analyzed by NMR spectroscopy. Assignment of the signals was carried out using two-dimensional spectra of ^1H-^1H COSY (Figs S35, S44, and S46 in the Supporting Information).

Single crystal X-ray studies

All crystals were obtained by recrystallization from acetonitrile. Recrystallization of **3** led to the crystals with the known unit cell parameters.[6] X-ray diffraction measurements were carried out using Bruker APEX II CCD diffractometer at 120 K. The frames were integrated and corrected for absorption by the APEX2 program package.[22] The details of crystallographic data and experimental conditions are given in Table S1. The structures were solved by the direct methods and refined by full-matrix least-squares technique against F^2 in the anisotropic-isotropic approximation. Hydrogen atoms were located from the difference Fourier maps and refined in rigid body model; the H(N) atoms were refined freely. All calculations were performed using the SHELX-2014[23] and Olex2[24] program packages. Crystallographic data for the structural analysis of **4**, **3**·$HClO_4$ and **4**·$(HClO_4)_2$ have been deposited with the Cambridge Crystallographic Data Centre, CCDC Nos. 1040937-1040939.

Quantum chemical calculations

Computational studies were carried out using the Gaussian09 program.[25] The structures of isolated molecules **3** and **4** were optimized using PBE0/6-311G(d,p) method/basis set with subsequent calculation of Hessian matrix. Optimized geometries of **3** and **4** are given in the Supporting Information.

Acknowledgements

The authors thank the financial support from RFBR for S. K. (complex formation study), A. P., and M. O. grant nos. 13-03-01304, 15-03-04695, and 14-03-31932 (synthesis of the crown ether ligands) for financial support.

REFERENCES

[1] J. S. Bradshaw, K. E. Krakowiak, R. M. Izatt, *Aza-Crown Macrocycles*Wiley, New York, **1993**.
[2] K. E. Krakowiak, J. S. Bradshaw, D. J. Zamecka-Krakowiak, *Chem Rev*. **1989**, *89*, 929–972.
[3] K. B. Mertes, J. M. Lehn, in: *Comprehensive Coordination Chemistry* (Eds: G. Wilkinson), , Pergamon, Oxford, **1987**.
[4] R. M. Izatt, J. S. Bradshaw, S. A. Nielson, J. D. Lamb, J. J. Christensen, *Chem Rev*. **1985**, *85*, 271–339.
[5] O. Fedorova, Y. Fedorov, M. Oshchepkov, M. Dobrovolskaya, *J Phys Org Chem*. **2012**, *25*, 835–839.
[6] I. V. Korendovych, R. J. Staples, W. M. Reiff, E. V. Rybak-Akimova, *Inorg Chem*. **2004**, *43*, 3930–3941.
[7] I. V. Korendovych, M. Cho, P. L. Butler, R. J. Staples, E. V. Rybak-Akimova, *Org Lett*. **2006**, *8*, 3171–3174.
[8] D. Grykoa, D. T. Grykoa, H. Sierzputowska-Gracz, P. Pia Atekc, J. Jurczak, *Helv Chim Acta*. **2004**, *87*, 156–166.
[9] I. V. Korendovych, M. Cho, O. V. Makhlynets, P. L. Butler, R. J. Staples, E. V. Rybak-Akimova, *J Org Chem*. **2008**, *73*, 4771–4782.
[10] P. Gans, A. Sabatini, A. Vacca, *Talanta*. **1996**, *43*, 1739–1753.
[11] A. A. Mohamed, G. S. Masaret, A. H. M. Elwahy, *Tetrahedron*. **2007**, *63*, 4000–4010.
[12] H. Miyake, *Symmetry*. **2014**, *6*, 880–895.
[13] J.-M. Suk, V. R. Naidu, X. Liu, M. S. Lah, K.-S. Jeong, *J Am Chem Soc*. **2011**, *133*, 13938–13941.
[14] M. Enamullah, A. K. M. R. Uddin, G. Pescitelli, R. Berardozzi, G. Makhloufi, V. Vasylyeva, A.-C. Chamayoud, C. Janiak, *Dalton Trans*. **2014**, *43*, 3313–3329.
[15] A. S. Fernandes, M. F. Cabral, J. Costa, M. Castro, R. Delgado, M. G. B. Drew, V. Felix, *Inorg Biochem*. **2011**, *105*, 410–419.
[16] B. Draho, J. Kotek, P. Hermann, I. Luke, Eva Toth. *Inorg Chem*. **2010**, *49*, 3224–3238.
[17] O. Fedorova, Y. Fedorov, M. Oshchepkov, *J Electroanalysis*. **2012**, *8*, 1739–1744.
[18] B. H. Northrop, F. Aric, N. Tangchiavang, J. D. Badji, J. F. Stoddart, *Org Lett*. **2006**, *8*, 3899–3902.
[19] R. Pribil, *Analytical Applications of EDTA and Related Compounds*, Pergamon Press, Oxford, New York, Toronto, Sydney, Braunschweig, **1972**.
[20] P. Gans, B. O`Sullivan. *Talanta*. **2000**, *51*, 33–37.
[21] R. F. Jameson, M. F. Wilson, *J Chem Soc Dalton Trans*. **1972**, *23*, 2607–2610.
[22] APEX2 software package, Bruker AXS Inc., 5465, East Cheryl Parkway, Madison, WI 5317, **2005**.
[23] G. M. Sheldrick, *Acta Cryst*. **2008**, *A64*, 112–122.
[24] O. V. Dolomanov, L. J. Bourhis, R. J. Gildea, J. A. K. Howard, H. Puschmann, *J Appl Cryst*. **2009**, *42*, 339–341.
[25] M. J. Frisch, G. W. Trucks, H. B. Schlegel, G. E. Scuseria, M. A. Robb, J. R. Cheeseman, G. Scalmani, V. Barone, B. Mennucci, G. A. Petersson, H. Nakatsuji, M. Caricato, X. Li, H. P. Hratchian, A. F. Izmaylov, J. Bloino, G. Zheng, J. L. Sonnenberg, M. Hada, M. Ehara, K. Toyota, R. Fukuda, J. Hasegawa, M. Ishida, T. Nakajima, Y. Honda, O. Kitao, H. Nakai, T. Vreven, J. A. Montgomery Jr. , J. E. Peralta, F. Ogliaro, M. Bearpark, J. J. Heyd, E. Brothers, K. N. Kudin, V. N. Staroverov, R. Kobayashi, J. Normand, K. Raghavachari, A. Rendell, J. C. Burant, S. S. Iyengar, J. Tomasi, M. Cossi, N. Rega, J. M. Millam, M. Klene, J. E. Knox, J. B. Cross, V. Bakken, C. Adamo, J. Jaramillo, R. Gomperts, R. E. Stratmann, O. Yazyev, A. J. Austin, R. Cammi, C. Pomelli, J. W. Ochterski, R. L. Martin, K. Morokuma, V. G. Zakrzewski, G. A. Voth, P. Salvador, J. J. Dannenberg, S. Dapprich, A. D. Daniels, Ö. Farkas, J. B. Foresman, J. V. Ortiz, J. Cioslowski, D. J. Fox, *Gaussian 09, Revision B.01*Gaussian, Inc., Wallingford CT, **2010**.

SUPPORTING INFORMATION

Additional supporting information can be found in the online version of this article at the publisher's website.